Three-Dimensional Reconstruction of Parenchymal Units in the Liver of the Rat

HARALD F. TEUTSCH, DIRK SCHUERFELD, AND ELKE GROEZINGER

To investigate the parenchymal units in the liver of the rat three-dimensionally, 15 μm cryosections were used for the demonstration of glucose-6-phosphatase (G6Pase) activity to visualize the borders of the individual units. Together with the supplying and draining vessels, they were traced through a sequence of 146 sections and reconstructed. A cone-shaped secondary unit with a height of 2.1 mm and a volume of 3.3 mm^3 was reconstructed. It was "covered" by a continuous vascular surface, consisting of portal tracts and vascular septa, connecting the portal venular branches. The secondary unit was subdivided by portal tracts and vascular septa, and by branches of a draining central venular tree into 14 primary units. Most of them were tri- to heptahedral in shape. The height varied between 330 and 840 μm, and the volume varied between 0.094 and 0.621 mm^3. The branches of the portal venular tree, with diameters from 28 ± 5 μm to 61 ± 14 μm, were oriented preferentially along the vertical axis of the units. Most of the primary units were drained by single branches of the central venular tree, located in the center and oriented along the vertical axis of the units. Vessel diameters ranged from 62 ± 14 μm to 216 ± 9 μm. The average length of the sinusoids was 355 ± 3 μm. From the results of this reconstruction study, it was concluded that the concept of the liver acinus cannot be applied to the liver of the rat. (HEPATOLOGY 1999;29: 494-505.)

The question of what constitutes the structural and functional unit of the liver has been for a long time, and still is today, a matter for debate. Various concepts have been proposed, such as that of the "classical lobule,"[1,2] the "portal unit,"[3] the "acinus"[4] and variations thereof,[5,6] and the "modified lobule."[7-10] In the rat, the three-dimensional structure and arrangement of the parenchymal unit and its supplying and draining vasculature are so far only partially understood,[8-11] and further investigation is required. Three-dimensional reconstruction appears adequate for investigating the subdivision of liver parenchyma into structural/functional units.

Whereas in the liver of the pig,[12-14] individual parenchymal units are separated by connective tissue and therefore can be distinguished without difficulty, this is not the case with the liver of the rat, and thus the problem of how to identify individual parenchymal units arises. In previous studies,[15,16] we have found that this problem can be solved by visualization of cell function with enzyme histochemical techniques, in particular by the demonstration of glucose-6-phosphatase (G6Pase) activity, because this clearly marks the perimeter of the parenchymal unit.

MATERIALS AND METHODS

Preparation of Materials. Three-month-old male and female Wistar rats (obtained from Charles River Breeding Laboratories Inc., Wilmington, MA) with an average body weight of 500 and 290 g, respectively, were maintained at a constant temperature (21°C) and under a light/dark cycle (light from 6 AM to 6 PM), and fed on a diet of Purina chow and water *ad libitum*. After 2 weeks of adaptation, the animals were anesthetized by intraperitoneal injection of sodium pentobarbital (5 mg/100 g body weight). After 30 minutes of anesthesia, during which time the animals were maintained at an ambient temperature of 37°C to allow for dissipation of stress,[17] the livers were frozen *in situ* with liquid nitrogen,[18] removed, and stored in liquid nitrogen until required. Serial cryosections (15 μm) were cut parallel to the convex surface of the left lobe[19] and used for the histochemical demonstration of G6Pase activity[20] to identify and delineate the individual parenchymal units. Before sectioning, the tissue samples were trimmed with a cutter (see below) so that the outlines of the sections could be used later for the vertical orientation of the section planes. Animal experiments were performed in compliance with the National Research Council's criteria for the care and use of laboratory animals in research.

To determine the degree to which the liver tissue was altered in its dimensions during sectioning, drying, and histochemical staining, the tissue blocks were trimmed with a cutter made out of two razor blades that had been mounted parallel to each other, using a metal spacer. The mounted tissue sample was trimmed to produce two cuts at right angles to each other. After processing the cryosections, they were photographed on Polaroid film, and the outlines of the sections were digitized and the tissue area calculated using a computer program (Histol, obtained from LIST-electronic, Darmstadt, Germany). A total of 25 sections were analyzed, and it was found that the shrinkage of the tissue amounted to 9% ± 3%, on average.

The diameters of the distributing branches of the portal vein were determined in cryosections stained histochemically for G6Pase activity. For this purpose, the sections were viewed in phase-contrast, the outlines of cross-sectioned vessels were documented on paper, and the vessel diameters measured at a magnification of 230:1, using a calibrated drawing tube attached to the microscope.

Three-Dimensional Reconstruction. From several series of sections, one series of 146 sections (from the liver of a female rat) was selected for the final reconstruction study and documented on

Abbreviation: G6Pase, glucose-6-phosphatase.

From the Department of Anatomy, University of Ulm, Germany.

Received June 8, 1998; accepted October 19, 1998.

Experiments were performed in part in the Department of Anatomy, West Virginia University, Morgantown, WV, when H.F.T. was Research Professor of Anatomy and Recipient of a Heisenberg Award from the Deutsche Forschungsgemeinschaft.

Supported by grants from the National Institutes of Health (grant AM32554-03) and the University of Ulm.

Address reprint requests to: Prof. Dr. Harald F. Teutsch, Department of Anatomy, University of Ulm, Albert-Einstein Allee 11, D-89069 Ulm, Germany. E-mail: harald.teutsch@medizin.uni-ulm.de; fax: 49-731-502-3214.

0270-9139/99/2902-0024$3.00/0

Polaroid film (Type 55). The photographs were then used to prepare drawings that contained the outlines of individual parenchymal units together with the portal tracts and draining vessels. Starting with the central venule of an individual parenchymal unit, at the surface of the liver, the central venular tree was followed to the point where it joined a sublobular branch of the hepatic vein. Finally, the vascular tree of supplying vessels (*i.e.*, portal veins) of the secondary unit was analyzed. The final set of drawings was digitized, using a computer program (Histol), for simple three-dimensional reconstruction and morphometric analysis. In addition, solid models were built. For this purpose, the individual drawings were transferred onto polystyrene sheets, cut with a wire cutter, and assembled. The surface of the models was smoothed with modeling clay and coated with epoxy resin.

Morphometric Analyses. The digitized set of drawings was analyzed with the Histol program, and the following morphometric values were determined for individual primary units: the height, the volume, the areas of the vascular septa, and the lengths of the sinusoids.

Calculation of the Volumes of Sinusoidal Segments and of Volume Gradients of G6Pase and Glucokinase Activities. In previous microchemical studies, where sinusoidal gradients of enzyme activity and metabolite levels had been determined, a subdivision of the sinusoidal length into six consecutive segments had been found to provide sufficient precision for the assessment of the metabolic heterogeneity of hepatocytes.[15,21] In those studies, enzyme activity was expressed as millimoles of substrate converted per unit of tissue, *i.e.*, liter of wet tissue. The present study offered the possibility of determining the volumes of the six sinusoidal segments, and then calculating the enzyme activity on the basis of the volumes of the different segments, whereby the "linear" gradients could be converted into volume gradients. For this purpose, all of the cross-sections of a primary unit (Fig. 1) were used, the lengths of the sinusoids being subdivided into six segments and the borders of the segments determined. The drawings were digitized and the volumes of the six segments of the various primary units were calculated. Units 10, 13, and 14 were not included because of their drainage by several central venular branches that did not permit the sinusoidal segments to be clearly defined. To investigate the value of such calculations, microchemical data on the distribution of the activities of G6Pase[17] and of glucokinase[18] in the livers of female rats in six consecutive segments along the sinusoid were used to determine the respective "volume-based" gradients. Statistical analysis used ANOVA and the Newman-Keuls test.[22]

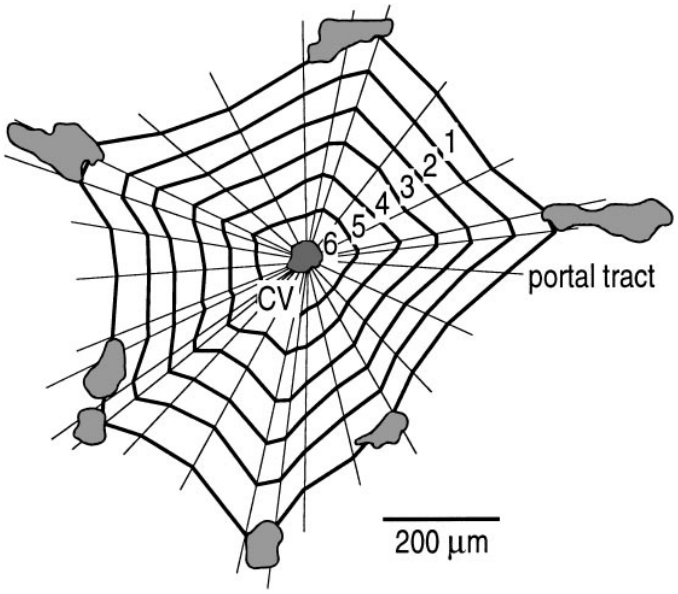

FIG. 1. Cross-section of a primary unit subdivided into 6 sinusoidal segments. The borders of the segments were determined by subdividing a number of radii (*thin lines*) into 6 equal parts and connecting corresponding partitions. 1-6: sinusoidal segments. Segment 1 comprises hepatocytes located at the beginning of the sinusoids; segment 6, surrounding the central vein, comprises hepatocytes at the end of the sinusoids. CV, central vein.

RESULTS

Distribution of G6Pase Activity. Figure 2A and 2B show the distribution of G6Pase activity in a cryosection and the corresponding drawing. Enzyme activity was demonstrated in the cytoplasm of hepatocytes; no specific reaction product was detected in nonparenchymal cells, the walls of portal vessels, bile ducts, or central veins. In general, high enzyme activity was located along the perimeter, and low activity was found in the center (around the central venules) of the cross-sectioned parenchymal units. Neighboring portal tracts and interconnecting sinusoids making up vascular septa form a continuum by which blood is distributed over the surface of the parenchymal units, and from which the sinusoids take their origin (Fig. 2B, unit 7). From portal tracts, blood flows along the vascular septa (Fig. 2B, *black lines*) in the direction indicated by *blue arrowheads*. Enzyme activity was highest in hepatocytes located at the beginning of "portal" sinusoids (Fig. 2A and 2B, unit 6) that originate directly and in the vicinity of the portal venules. From there, it decreased in the direction of the central venule. A second gradient was found between neighboring portal tracts, where staining decreased from both sides (with the direction of blood flow) along the vascular septum, and was lowest in the area indicated by the position of the arrowheads, where the "septal" sinusoids originate (Fig. 2A and 2B, units 1 and 3). From there, enzyme activity decreased along the axis of the septal sinusoids and was lowest in hepatocytes located at the central venule.

General Organization of the Parenchyma. Tracing the portal tracts and vascular septa and the draining vessels (Fig. 3) through a sequence of 146 sections revealed a group of simple (primary) units integrated into one larger (secondary) unit. This integration resulted from a common drainage by all the branches of one particular central venular tree (Fig. 4C and 4D), and from the arrangement of portal tracts and vascular septa that form a continuous vascular surface over the entire unit and separate it from adjacent units (Fig. 4A and 4B). The secondary unit was cone-shaped, and it had a height of 2.1 mm and a parenchymal volume (excluding the volume of the supplying and draining vessels) of 3.330 mm^3 (3,330 nL). The oval base, with a major axis of 2.92 mm and a minor axis of 1.59 mm, was located adjacent to the upper convex surface of the left lobe. At the apex, pointing away from the surface, the supplying vascular surface had an opening through which the stem of the central venular tree was connected to a sublobular branch of the hepatic vein.

The parenchyma of the secondary unit was subdivided internally by portal tracts and vascular septa originating from the supplying vascular surface, and by branches of the central venular tree, into primary units. The number of primary units decreased from the base to the apex. Thus, there were 8 units at the base (Fig. 3, 45 µm). The number was consecutively reduced to 6 at 495 µm below the top surface, to 5 at 735 µm, to 4 at 885 µm, to 3 at 1,230 µm, and finally to 1, starting at 1,320 µm below the lobar surface.

The reduction of the number of primary units resulted from connecting two adjacent units, in the course of which the "separating" vascular septum ended, followed at a distance by the fusion of the central venular branches of the two

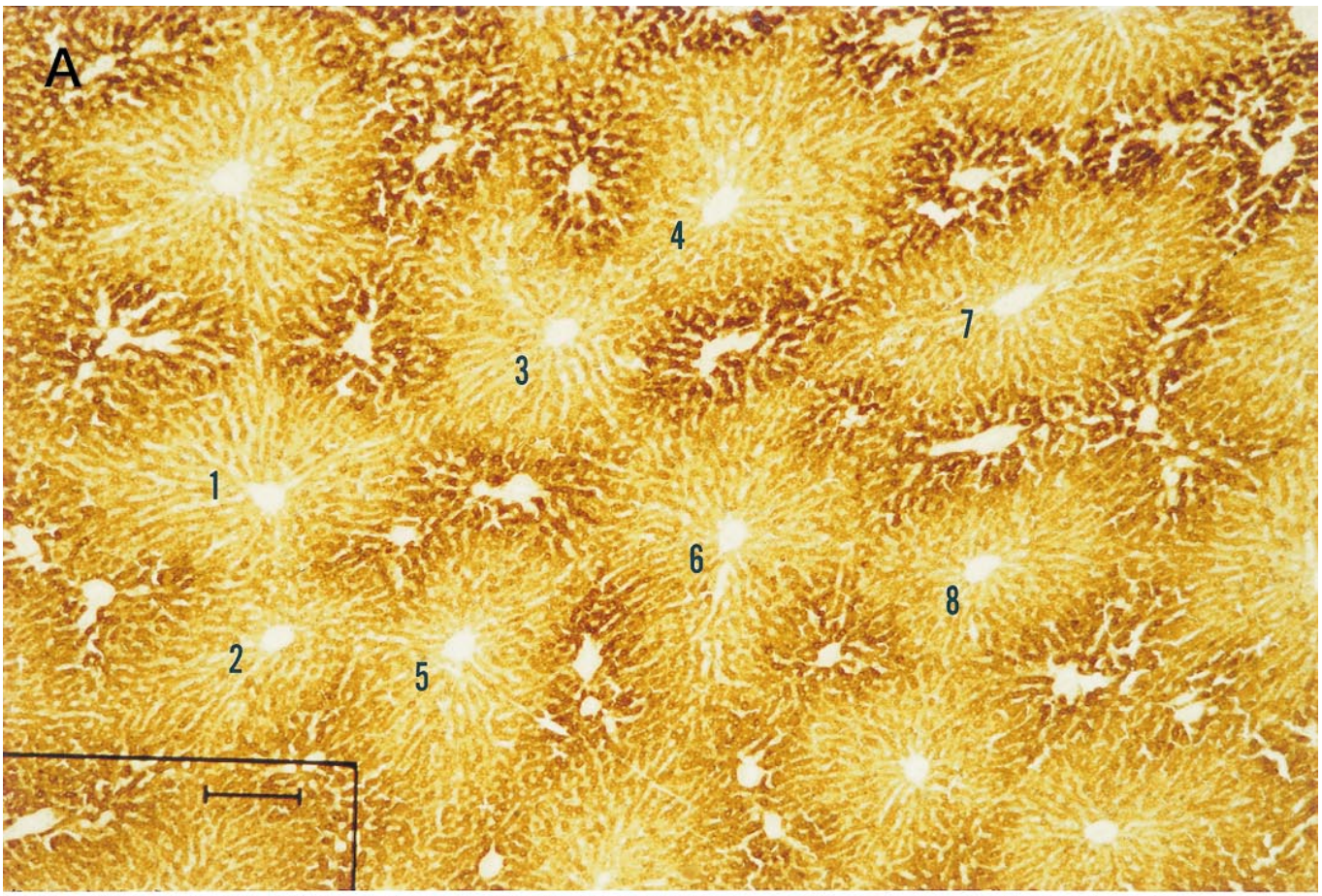
A
1
2
3
4
5
6
7
8

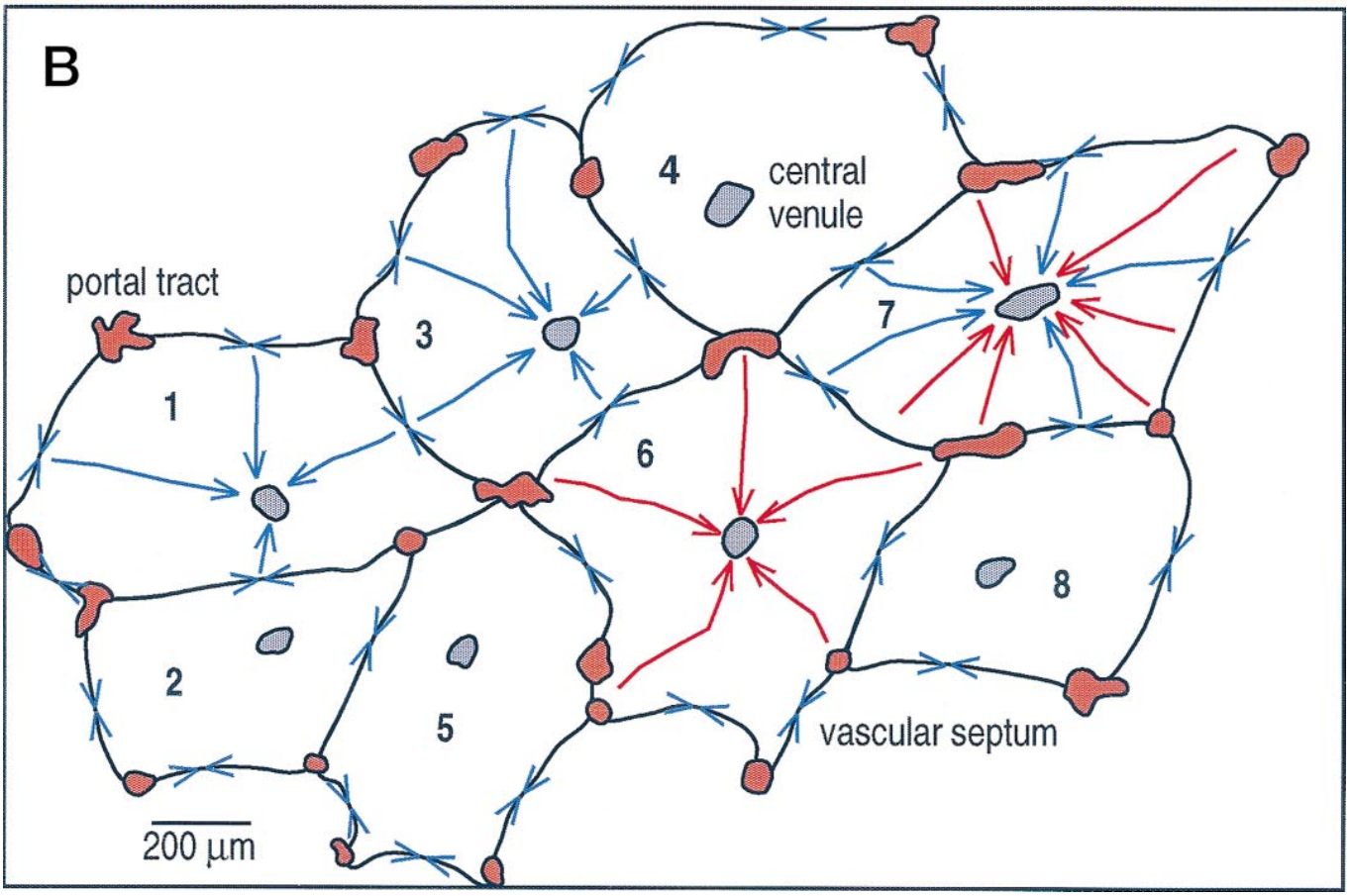
B
portal tract
central venule
vascular septum
1
2
3
4
5
6
7
8
200 µm

units involved. This distance was found to be 167 ± 20 (± SEM, 9 measurements) μm on average. The explanation as to why this distance was shorter than the average length of sinusoids of 355 ± 3 (± SEM, 1,300 measurements) μm, relates to the observation that sinusoids located between the vascular septum and the bifurcation of the central vein were not, in most cases, sectioned along their longitudinal axis, but at variable angles, thus reducing the apparent length of the sinusoids.

The Central Venular Tree. The central venular tree, draining the secondary unit (Figs. 4C, 4D, and 5A), was oriented perpendicular to the organ surface. Most of the beginnings of the initial tributaries were located about 50 μm below the surface, and the junction of the vascular stem with the sublobular vein was located at a distance of 2.1 mm from the surface. Based on the diameter of the vessels, 4 types of branches could be distinguished: the main stem (14) with an average diameter of 216 ± 9 (± SEM) μm, one type 2 branch (12) with a diameter of 171 ± 18 μm, 3 type 3 branches (9, 10, 11) with a diameter of 111 ± 10 μm, and 15 type 4 branches (1-8, 10/1, 13/1-3, 14/1-3) with an average diameter of 62 ± 14 μm, 7 of which resulted from the fusion of two short initial segments. The branching of the draining vascular tree was mostly asymmetrical. The main vessel (14) received three type 4 vessels (14/1-3), one type 2 (12), and one type 3 vessel (11). The latter divided into two type 4 branches (7, 8). The type 2 vessel (12) divided into two type 3 vessels (9, 10) and two type 4 vessels (5, 6). The type 3 vessel (10) further divided into three type 4 vessels (3, 4, 10/1); the other (9) gave off five type 4 branches (1, 2, 13/1-3). The majority (12 of 14) of the units were drained by a single branch of the central venular tree. Unit 10 was drained by one type 3 vessel and one very short type 4 vessel (10, 10/1); unit 13 was drained by three type 4 vessels (13/1-3), and unit 14 was drained by the main vessel (14) and three type 4 vessels (14/1-3).

Portal Venous Trees. The secondary unit was supplied by three portal veins (Figs. 3, 4A, 4B, 5B), one (p2) in the middle, one on its right side (p1), and one (p3) on its left side. Similar to the branching of the central venous tree, 4 types of branches could be distinguished (Fig. 5B): the largest vessel (p2) with an average diameter of 61 ± 14 (± SEM) μm, 6 type 2 branches with a diameter of 48 ± 9 μm (Fig. 5B: 12, 21-24, 30), 17 type 3 branches with a diameter of 35 ± 7 μm, and 38 type 4 branches with a diameter of 28 ± 5 μm, 3 of which further divided (without reduction of the vessel diameter) into 7 additional branches with a diameter of 27 ± 5 μm. From a total of 62 branches of portal veins, 55 were located at the "lateral" surface of the secondary unit, and 7 branches were found to supply blood to the "internal" surfaces of the primary units (Fig. 5B, branches marked with *asterisks*). The majority of type 4 branches terminated at a distance of 200 to 250 μm away from the top surface.

Organization of the Secondary Unit. By tracing the internal subdivision of the secondary unit, 4 groups, consisting of 3 to 4 units each, and 1 single unit were detected (Figs. 4A, 4B, 6).

The schematic drawing (Fig. 6A) shows that group A consisted of units 1, 2, 9, and 13 that were arranged in three layers, on the left side of the secondary unit (Fig. 4A). The portal blood supply (Fig. 7, a1-a4) came from 3 type 2 branches (21, 22, 30) dividing at rather small angles into 4 type 3 and 9 type 4 branches, oriented along the vertical axis and determining the edges of the primary units. The vascular septa, connecting neighboring portal vessels, received additional blood supply through short type 4 vessels branching off mostly at sharp angles. Units 1 and 2 were located adjacent to the lobar surface and drained by single branches of the central venular tree. The vascular septum between these units ended 315 μm below the top surface, the central venules joined at a depth of 450 μm. The units were 450 μm high. Unit 1 had 4 faces at the top and 3 faces at the base, with a surface (*i.e.*, mantle) area of 0.932 mm^2 (Table 1) and a volume of 0.094 mm^3 (Table 2); unit 2 had 6 faces at the top and 5 faces at the base, with a surface area of 1.199 mm^2 and a volume of 0.155 mm^3. Unit 9, located below units 1 and 2, was drained by a single central venule and ended (fusion of the central venule with that of unit 13 and that of unit 5 of group b) 780 μm below the lobar surface. It was 330 μm high, and had 5 faces with a total area of 1.037 mm^2 and a volume of 0.156 mm^3. With regard to blood flow, unit 13 was positioned in the opposite direction, *i.e.*, it began at a depth of 1,275 μm. It was drained by three branches of the central venular tree. The vascular septum between unit 13 and unit 12 of group b extended from a depth of 1,275 μm to 915 μm. Unit 13 had a height of 495 μm, with 4 faces toward unit 9 and 6 faces at a depth of 1,275 μm, and a total area of 1.660 mm^2 and a volume of 0.282 mm^3.

Group b consisted of units 5, 6, and 12, arranged in two layers, located in the middle of the secondary unit (Figs. 4A and 6B). It was supplied by 3 type 2 vessels (21, 24, 22) branching into 5 type 3 and 11 type 4 vessels (Fig. 7, b1-4). The portal vessels 21 and 24 ran in an oblique direction; the other branches were oriented close to the vertical axis. As in group a, there were additional short, mainly horizontal branches supplying the vascular septa. Units 5 and 6 were located adjacent to the lobar surface. The vascular septum between these units ended 630 μm below; the central venules joined at 780 μm. The units had 7 faces at the top and 3 faces at the base, with total mantle areas of 1.696 and 2.597 mm^2 (Table 1) and volumes of 0.202 and 0.318 mm^3, respectively. Unit 5 and unit 9 were connected at 780 μm below the lobar surface by the fusion of their central venules. The end of the septum between units 5 and 9 of group a was located at a distance of 495 μm from the top. Unit 12, located below units 5 and 6, ended at 1,320 μm with the fusion of the central venule with that of unit 11 of group c. The vascular septum between units 11 and 12 ended at a depth of 1,095 μm. Unit 12 was 540 μm high, and had 6 faces toward units 5 and 6 and 4 faces towards unit 14, with a total mantle area of 1.763 mm^2 and a volume of 0.260 mm^3.

FIG. 2. (A) Distribution of G6Pase activity in the liver of a female rat. Enzyme activity is highest in hepatocytes located at the beginning of "portal" sinusoids (*red arrows* in [B]) and decreases toward the central venule. A second gradient is present along the vascular septum, where enzyme activity decreases from neighboring portal tracts toward the "middle" of the septum (*blue arrowheads* in [B]). From there, enzyme activity decreases along "septal" sinusoids (*blue arrows* in [B]) and is lowest in hepatocytes located at the central venule. (B) Schematic drawing of 8 adjacent primary units according to the distribution of G6Pase activity shown in (A). Portal tracts and vascular septa are located along the perimeter of polygonal cross-sections of primary parenchymal units (1-8), where sinusoids take their origin. In unit 7, *arrows* indicate the direction of sinusoidal blood flow from the perimeter toward the draining central venule. According to the origin, two types of sinusoids can be distinguished: "portal" sinusoids, originating directly from and in the close vicinity of portal venules (*red arrows* in unit 6), and "septal" sinusoids, originating from that location along the vascular septa, where flow fronts meet (*blue arrows* in units 1 and 3). *Arrowheads* indicate the direction of blood flow along the vascular septa. The position of the *arrowheads* indicates where the flow fronts from neighboring portal tracts meet.

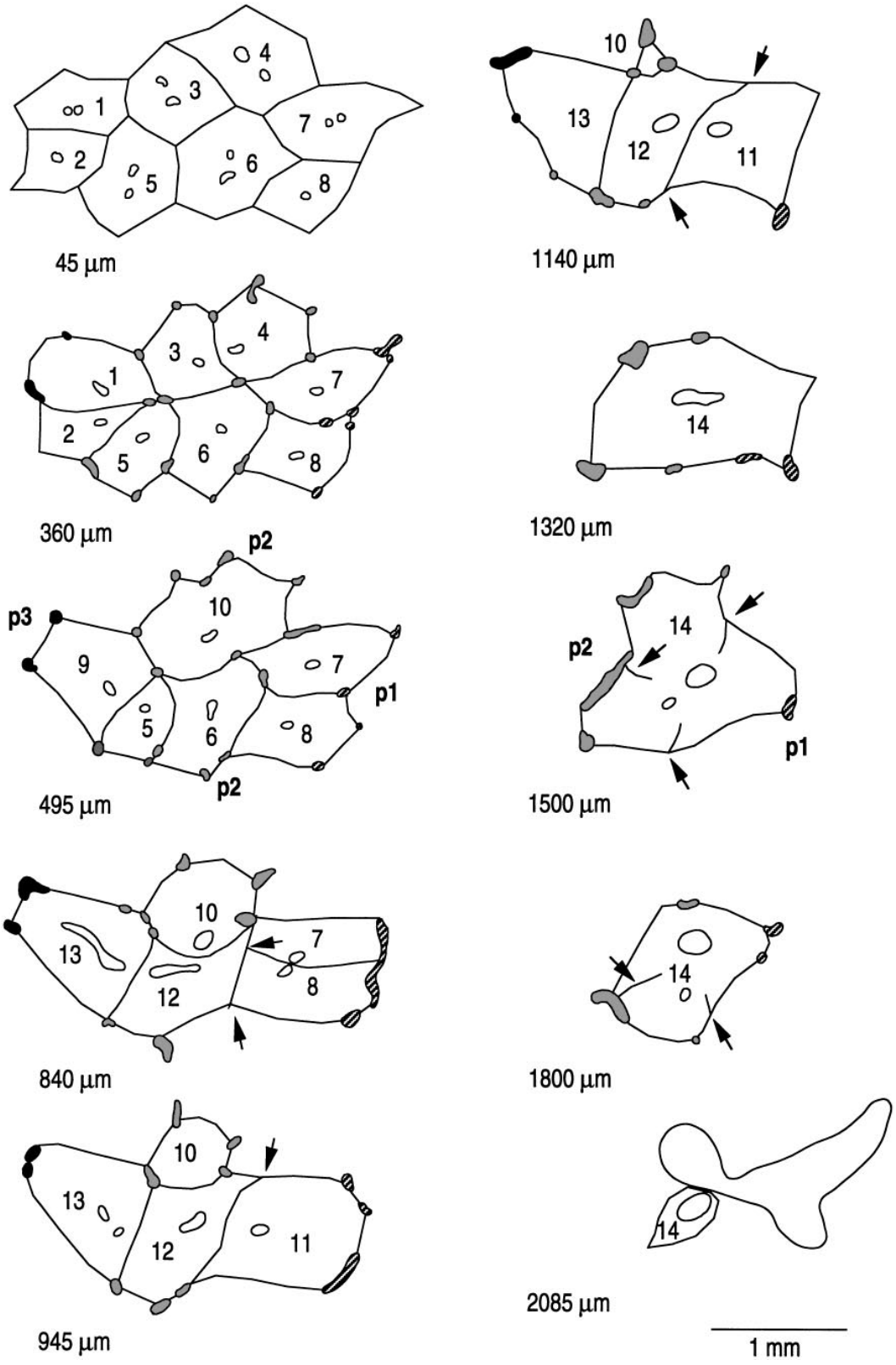

FIG. 3. Drawings of representative section planes of a series of 146 sections showing the secondary parenchymal unit and its subdivision by portal tracts (p1: areas shaded in *black*, p2: areas shaded in *gray*, p3: *hatched* areas), vascular septa, and branches of the central venular tree in the center of primary units (*open circles*) into 14 primary units. *Numerals* at the lower left side of the drawings indicate the distance of the section plane from the top surface. *Other numerals* indicate individual primary units. *Arrows* in section planes 840, 945, 1,140, 1,500, and 1,800 µm point to areas where the vascular septum divides and/or is connected only on one side to a portal tract or a septum.

Group c comprised the units 7, 8, and 11, which were arranged in two layers, located on the right side of the secondary unit (Figs. 4A and 6C). It received its blood supply from 3 type 2 vessels (21, 12, 24), giving off 6 type 3 and 12 type 4 branches (Fig. 7, c1-4). The portal vessel 12 had a horizontal orientation, and it divided into type 3 and type 4 vessels following a mainly vertical direction. The branches of vessel 24 diverged at relatively small angles from the vertical axis. Blood supply to the "left edge" of units 8 and 11 (Fig. 7, c1 and right side of c4) through the branches of vessel 21 was discontinuous. As can also be seen from Fig. 4A, the borders (*i.e.*, vascular septa) of units 8 and 11 only extended in some

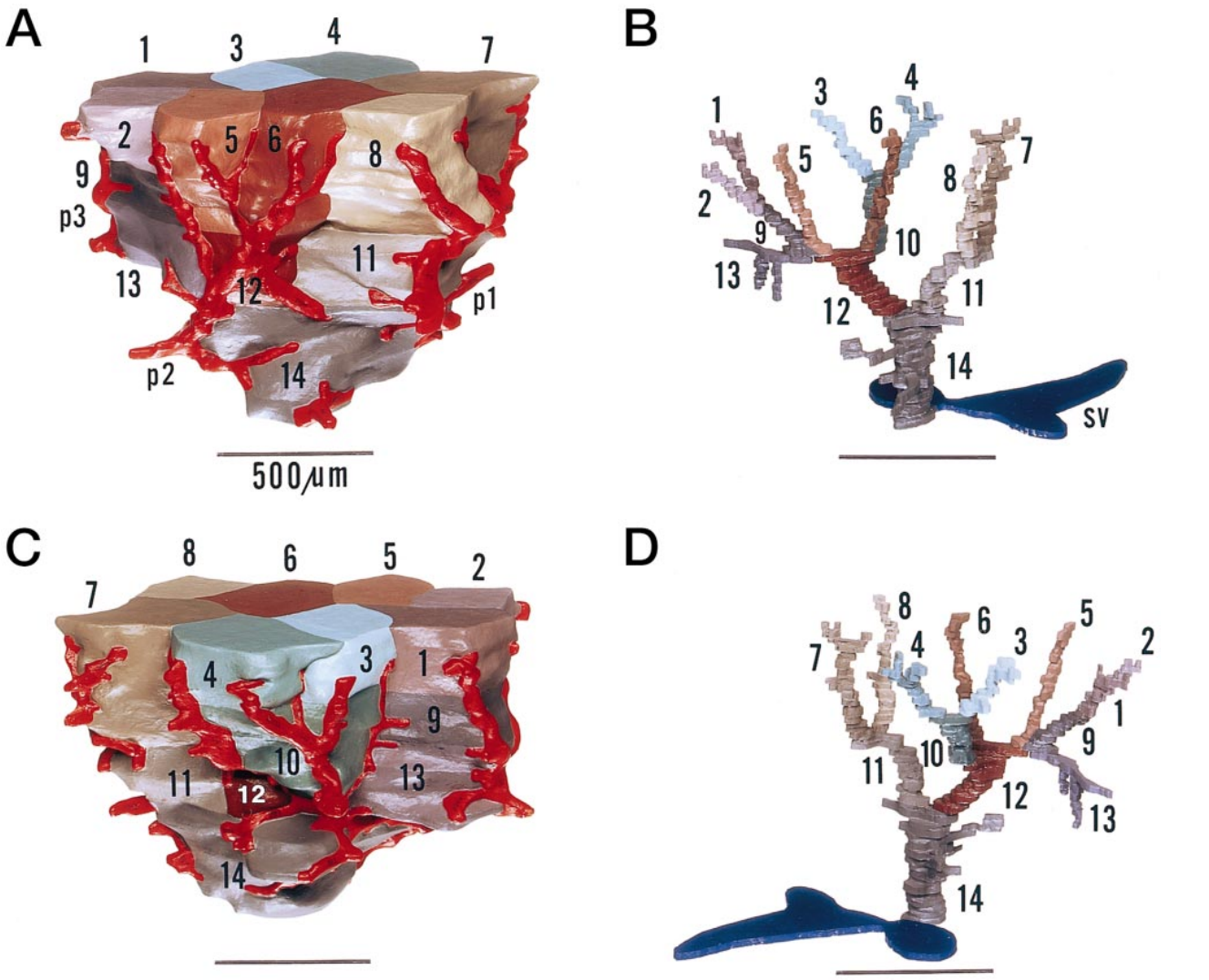

FIG. 4. Three-dimensional reconstruction of the secondary parenchymal unit and of the draining central venular tree. (A) Front view of the secondary unit. (B) Back view. *Numerals* indicate the primary units that are color-coded. Portal tracts are marked in *red* (p1, p2, p3). (C) Front view of the draining central venular tree. (D) Back view. *Numerals* indicate the different central venular branches that are color-coded to correspond to the primary units. The stem of the central venular tree empties into a sublobular vein (sv).

areas to the supplying portal vessels, whereas in other areas, units 8 and 11 terminated at a distance away from the supplying vessels. Cross-sections (Fig. 3) revealed in these areas a branching of the vascular septum.

Units 7 and 8 were located adjacent to the lobar surface and ended with the fusion of the central venules at 840 µm; the vascular septum ended at 735 µm. Units 7 and 8 had 5 faces at the top and 4 faces towards unit 11 with mantle areas of 2.417 and 2.102 mm^2 (Table 1) and volumes of 0.332 and 0.254 mm^3 (Table 2). Unit 11, located below units 7 and 8, ended at 1,320 µm with the fusion of the central venule with that of unit 12. The vascular septum between these units ended at a depth of 1,095 µm. Unit 11 had a height of 480 µm, it had 5 faces towards units 7 and 8 and 4 faces towards unit 14, a mantle area of 1.688 mm^2 and a volume of 0.292 mm^3.

Group d consisted of 3 units (3, 4, 10) arranged in two layers, and was located behind group b (Figs. 4B and 6D). Unit 3 was in contact with units 1, 5, and 6; unit 4 was in contact with units 6 and 7; and unit 10 was in contact with units 5, 6, and 12.

The primary units of this group were supplied by 3 type 2 vessels (22, 23, 24), branching at relatively small angles into 5 type 3 and 8 type 4 branches (Fig. 7, d1-4). In addition, there were 3 short horizontal branches supplying the vascular septa. Units 3 and 4 reached the lobar surface; their common vascular septum ended at 315 µm below and their central venules joined at a depth of 405 µm. Units 3 and 4 had 6 faces at the top and 5 faces toward unit 10, with mantle areas of 1.020 and 1.112 mm^2 and volumes of 0.137 and 0.162 mm^3, respectively. Unit 10 located below units 3 and 4 extended to a depth of 1,140 µm. The central venule joined with that of unit 12 of group b at 885 µm. Above this junction, the vascular septum between units 10 and 5 and 6 of group b ended at a depth of 630 µm; the septum between units 10 and 12, below the junction, extended from a depth of 1,140 µm to 1,005 µm. Unit 10 had a height of 735 µm and a volume of 0.254 mm^3; it was cone-shaped with 3 faces at the apex and 8 faces toward units 3 and 4, and a mantle area of 1.952 mm^2.

Unit 14 (Figs. 4A, 4B, 6E), the top of the cone-shaped secondary unit, ended at a depth of 2,085 µm with the

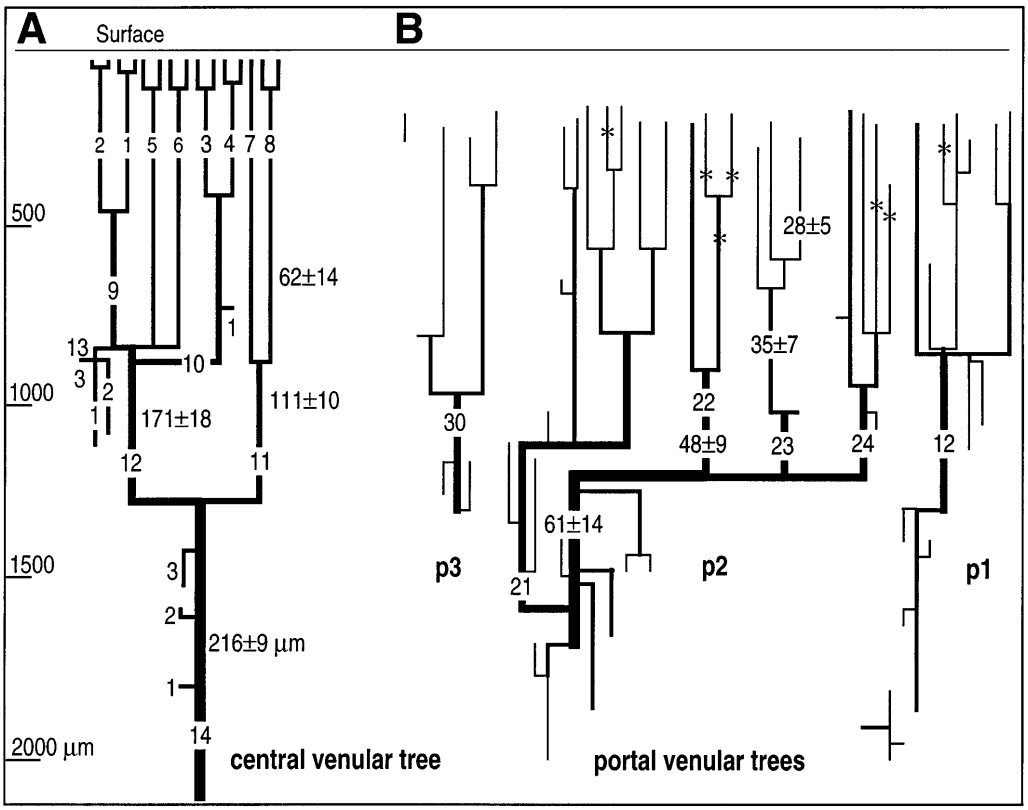

FIG. 5. (A) Schematic representation of the central venular tree draining the secondary unit. *Numerals* at the branches represent the mean diameters ± SEM of 4 types of central venular branches. *Other numerals* identify the individual branches of the central venular tree. Vertical scale: distance from the lobar surface. (B) Schematic representation of the portal venular trees (p1, p2, p3) supplying the secondary unit. Lines marked with *asterisks* represent branches located within the unit; the others are located at the lateral surface of the unit. *Numerals* at the branches represent the mean diameters ± SEM of the 4 types of portal venular branches. *Other numerals* identify branches of the portal venular trees.

junction of the main stem of the central venular tree with a sublobular hepatic vein. Unit 14 was supplied by 1 type 1 (Fig. 7, e1-4: 2) and 1 type 2 vessel (21), 6 type 3, and 8 type 4 vessels. In contrast to the portal vessels of groups a-d, the supplying vessels of unit 14 were oriented closer to a horizontal axis than to the vertical axis. Unit 14 was partially subdivided by 3 vascular septa and corresponding small additional central venular branches (Fig. 3, levels: 1,500, 1,800 µm). The unit had a height of 765 µm and a volume of 0.621 mm^3; it was cone-shaped with 3 faces at the apex and 7 faces toward units 11 and 12, and a mantle area of 3.016 mm^2.

Overall, the primary units were, with the exception of units 10 and 14, tri- to heptahedral (*i.e.*, 3 to 7 vascular septa), with areas between 0.031 and 0.703 mm^2 (Table 1), and mantle areas between 0.932 and 3.016 mm^2. The height varied between 330 and 840 µm, and the volume varied between 0.094 and 0.621 mm^3 (Table 2). The sinusoids had an average length of 355 ± 2 (± SEM, 1,300 measurements) µm. Portal sinusoids with 383 ±3 (± SEM, 640 measurements) µm were longer than septal sinusoids with 326 ± 2 (± SEM, 660 measurements) µm.

According to the analysis of 11 primary units (Table 2), the volumes of the sinusoidal segments 1 to 6 were 61 ± 7, 49 ± 6, 40 ± 5, 31 ± 4, 21 ± 3, and 13 ± 2 nL, on average (± SEM). Segments 1 to 5 were on average (± SEM) larger than segment 6 by factors of 4.9 ± 0.2, 4.0 ± 0.1, 3.2 ± 0.1, 2.5 ± 0.1, and 1.7 ± 0.0.

Comparison of Linear and Volumetric Gradients of G6Pase and Glucokinase Activity. According to the linear gradients (Fig. 8), G6Pase activity was highest at the beginning of the sinusoid (segment 1), decreased along the sinusoidal axis, and was lower by a factor of 1.7 (Fig. 8: S1/6 = 1.7:1) in segment 6 at the end of the sinusoid than was the activity of segment 1 (the values of segments 1 to 3 were significantly higher than those of segments 5 and 6). Glucokinase activity, on the other hand, was lowest in segment 1 and increased by a factor of 3.4 (Fig. 8: S6/1 = 3.4:1) along the sinusoid (the value of segment 1 was significantly lower than those of segments 4 to 6; those of segments 2 and 3 were significantly lower than those of segments 5 and 6).

Calculation of enzyme activity on the basis of the volumes of the segments had an opposite effect on these antagonistic enzymes: for G6Pase, it led to considerably higher differences among the segments, the values decreasing along the sinusoidal axis by a factor of 8.1 instead of 1.7 (significantly higher values were found in segment 1 as compared with segments 2 to 6, in segment 2 as compared with segments 3 to 6, in segment 4 as compared with segments 5 and 6, and in segment 5 as compared with segment 6), whereas for glucokinase, it resulted in similar activities in all of the segments (no significant differences were found). As can be seen from the addition of the segmental activities, the total G6Pase activity was 81 nmol per 215 nL of wet tissue per hour (equivalent to 377 mmol/L of wet weight per hour). Total glucokinase activity of the parenchymal unit was 17 nmol per 215 nL of wet tissue per hour (*i.e.*, 79 mmol/L wet tissue per hour).

DISCUSSION

The present study is based on previous histo- and microchemical investigations on the metabolic heterogeneity of hepatocytes and the functional integration of hepatocytes into parenchymal units.[15-17,21,23] From these studies, evidence has been accumulating against various aspects of the concept of an acinar unit[4] and its subdivision into 3 distinct metabolic zones,[24] and against the derived concept of a metabolic zonation.[25] Further criticism has come from other investigators.[8-10,26-28] In this context, the studies of Matsumoto et al.[28] and Matsumoto and Kawakami[7] on the angioarchitecture of the human liver were of particular relevance for the analysis of enzyme distribution in the liver of the rat.[15,16,23] This is

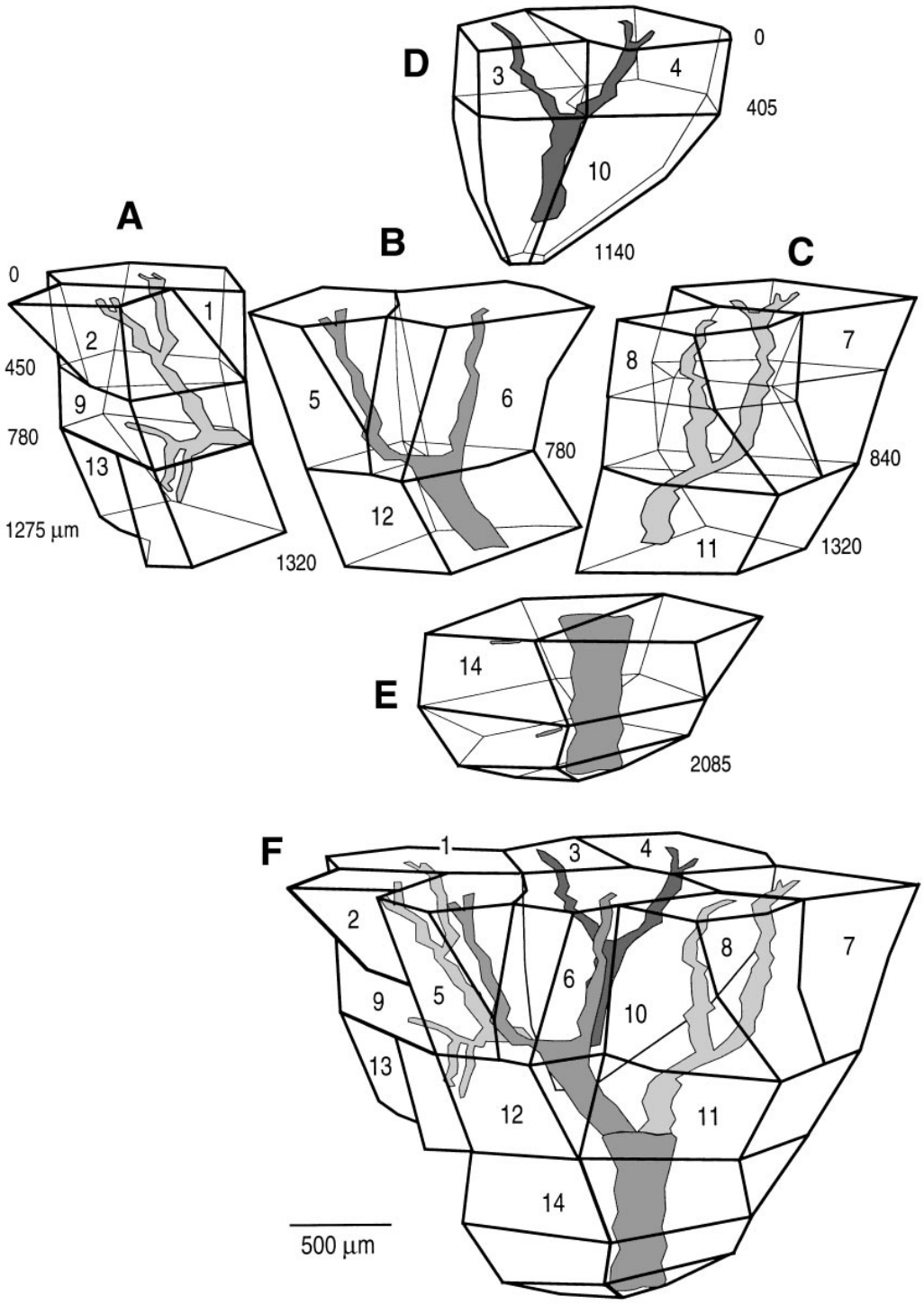

FIG. 6. Graphic representation of the organization of the secondary unit. Arrangement of primary units (1-14) into groups (A, B, C, D) according to the portal tracts and vascular septa, and drainage by central venules (shaded in *gray*). (E) single unit 14. (F) position of groups within the secondary unit. *Numerals* alongside the drawings indicate the distance (in µm) of the horizontal borders of the primary units from the lobar surface.

true, in particular, for the results of three-dimensional reconstructions, according to which neighboring portal venules and their septal branches are connected by vascular septa. These are composed of sinusoidal loops, from which blood is distributed to the sinusoids on both sides of the septum. Because of the specific morphology and arrangement of the sinusoids, the vascular septum acts like a "watershed" between adjacent parenchymal units. Portal venules and vascular septa make up a continuous supplying surface from which sinusoids originate. On the basis of these findings in the human liver, it was also possible to identify the vascular septa in sections of rat liver.[23] The distribution of enzyme activity was found to vary not only with the position of hepatocytes along the sinusoidal axis, but also with the origin of sinusoids,[15,16] *i.e.*, either directly from or in the near vicinity of portal venules (portal sinusoids), or from that area of the vascular septum where the blood flow fronts of neighboring portal venules meet (septal sinusoids). The distinction of portal and septal sinusoids is pragmatic insofar as it does not account for enzyme gradients along the septum, *i.e.*, the transition from typical portal to typical septal sinusoids.

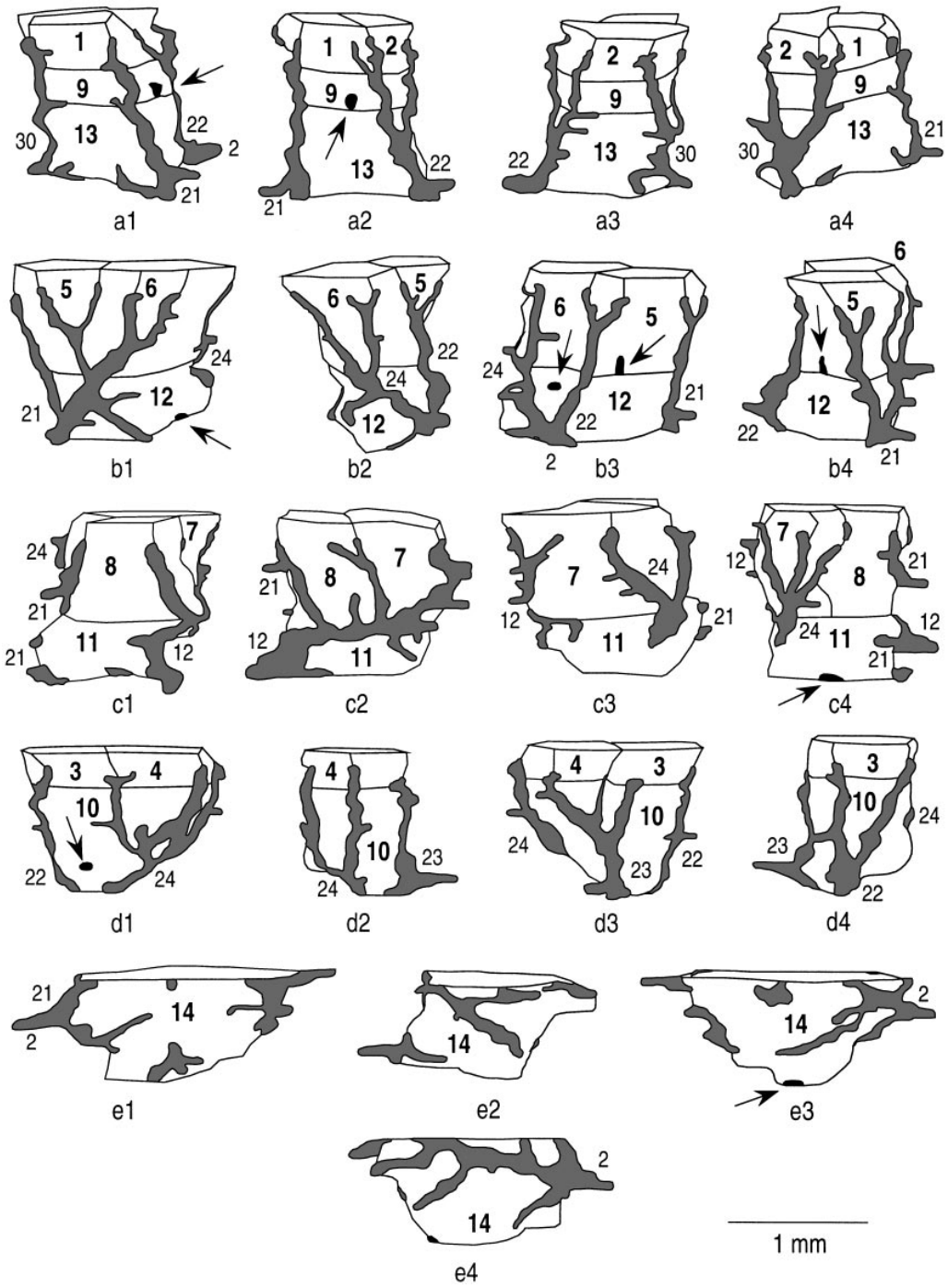

FIG. 7. Drawings from three-dimensional reconstructions of groups A, B, C, and D of primary units and of unit 14. The *numeral 1* (*e.g.*, a1) represents the position of the primary units in the secondary unit viewed from the front; *2-4* represent views obtained after counterclockwise rotation. Primary units are identified by *large numerals* as in Fig. 6. *Small numerals* indicate branches of portal tracts (shaded in *gray*) according to Fig. 5B. Small areas shaded in *black* and marked with *arrows* represent sectioned branches of the central venular tree. The central venule of unit 9 (Fig. a1 and a2) connects with that of unit 5 (Fig. b3 and b4), that of unit 6 (Fig. b3) connects with unit 10 (Fig. d1), that of unit 12 (Fig. b1) connects with that of unit 11 (Fig. c4). The small *black* area in unit 14 (Fig. e3) indicates where the main stem of the central venular tree exits from the secondary unit, *i.e.*, connects to the sublobular vein.

In the literature, the vascular septum and its importance for the blood supply to the parenchymal unit has already been discussed by Kiernan,[1] Debeyre,[29,30] and Pfuhl.[31] The radial arrangement, *i.e.*, the convergence of sinusoids toward the draining central venule, implies that portal blood must be distributed from the portal tract over a (sufficiently) large surface area to ensure blood supply to all of the sinusoids. This requirement is met by the vascular septa.

To our surprise, the three-dimensional reconstruction of the supplying portal vascular tree in the liver of the rat did not reveal any evidence for the presence of typical septal branches, branching off at a sharp angle from larger parent venules, as described by Pfuhl[32] and Matsumoto and Kawakami[7] in human liver, and Wuensche and Preuss[33] in the liver of the pig. In the rat, those additional branches to the vascular septa with mainly horizontal orientation were much too short and too few in number to be considered equivalent to the septal branches of human and pig liver. In Rappaport's concept,[4,24] these septal branches, *i.e.*, terminal afferent venules, are of considerable importance, because they represent the central axis of blood supply to the acinus. The absence of "true" septal branches therefore makes it difficult to apply this concept to the liver of the rat. This is also true for its newer versions,[5,6] in which, according to the schematic two-dimensional representation, not even two neighboring acini can be fitted between the supplying and draining

TABLE 1. Morphometric Data on Primary Units

Unit	Height (μm)	Faces	Areas of Vascular Septa (mm^2)							Total (mm^2)
1	450	3-4	0.180	0.194	0.245	0.313				0.932
2	450	5-6	0.095	0.097	0.213	0.235	0.242	0.317		1.199
9	330	5	0.110	0.140	0.244	0.255	0.288			1.037
13	495	4-6	0.162	0.170	0.184	0.261	0.394	0.489		1.660
5	780	3-7	0.036	0.069	0.097	0.186	0.285	0.502	0.521	1.696
6	780	3-7	0.295	0.300	0.323	0.332	0.369	0.456	0.522	2.597
12	540	4-6	0.144	0.167	0.240	0.287	0.442	0.484		1.763
7	840	4-5	0.285	0.326	0.549	0.554	0.703			2.417
8	840	4-5	0.127	0.401	0.438	0.556	0.580			2.102
11	480	4-5	0.083	0.316	0.402	0.440	0.446			1.688
3	405	5-6	0.037	0.147	0.185	0.189	0.227	0.235		1.020
4	405	5-6	0.031	0.160	0.216	0.221	0.238	0.246		1.112
10	735	3-7	0.082	0.106	0.185	0.254	0.266	0.445	0.614	1.952
14	765	3-7	0.083	0.089	0.095	0.225	0.519	0.587	0.680	3.016

vasculature without either overlapping of the units or leaving parenchymal areas undefined. This is also true for a three-dimensional assembling of berry-shaped (acinar) units.

The idea of a unit, in which the supplying portal vessels are located in the center and the draining vessels in the periphery, goes back to the concept of the portal unit,[3] which was also developed on the basis of studies on the livers of dogs and rabbits. In contrast to the acinar concept, the portal blood supply is assumed not to be provided by a terminal afferent portal venule, branching off at a sharp angle from the parent portal vein in the portal tract, but the terminal branch of the portal vein is thought to continue the direction of the portal tract, leading to a different orientation of the units, comparable with that of lobular units. In Mall's article, the portal units are depicted as polygons, and not as triangles, as represented in many textbooks, *e.g.*, Welsch[34] and Bucher,[35] and do, at least in a two-dimensional schematic representation, fit into the framework of the supplying and draining vasculature without overlapping or leaving parenchymal gaps. Nevertheless, Mall's and Rappaport's idea of a central axis of blood supply creates the problem of how the blood is drained from a large number of sinusoids into a small number of central venules. This requires, as can be seen from Mall's schematic drawing,[3] that the sinusoids first diverge from the central supplying portal vessel and then change their direction and converge toward the draining vessels located at the perimeter of the unit. As a consequence, the sinusoids vary considerably in length and are bent at variable angles, features that are not to be observed in tissue sections and that would counteract coordinated sinusoidal blood flow. While Mall[3] and Rappaport et al.[4] have restricted the blood supply to the sinusoids to the terminal branches of the portal venular tree, our reconstruction studies demonstrated that this is not the case in rat liver, but that portal venules with diameters from 28 to 61 μm (type 1-4 vessels) supply blood to the sinusoids. From the fact that a considerably larger portion of the portal venous tree in rat liver is involved in the blood supply to the sinusoids, it follows that the concepts of the acinus and the portal unit cannot be applied. Recently, Bhunchet and Wake[11] suggested a portal lobule in the liver of the rat, on the basis of results from dye injections into the portal and hepatic vein, and from analysis of thick translucent sections, resembling the portal unit described by Mall.[3]

The cone-shaped secondary unit reconstructed in this study is covered by a continuous supplying surface of portal vessels and vascular septa; only at the apex of the unit, where the stem of the central venular tree is connected to the sublobular vein, is there an opening. The secondary unit is subdivided into 4 groups of 3 or 4 primary units and 1 large single unit that is only partially subdivided. The subdivision results from the arrangement of portal vessels located within the secondary unit, originating from parent vessels at the lateral surface, and of vascular septa. From a total of 62 portal venular branches, only 7 are located within the unit and responsible for the internal subdivision. The small number of "internal" vessels can be explained by the fact that up to 4 vascular septa can be connected to a single portal vein branch. Although this study does not provide information on the so-called "inlet venules,"[36,37] it seems feasible to assume that they may be of importance for directing blood from the supplying portal vein to the different vascular septa connected to it. The height and width of the vascular septa vary with the position of neighboring portal venular branches. The septa are narrow at bifurcations and can be as wide as 1,000 μm between distal branches of the portal vein. While in most cases, the vascular septum is connected to and supplied by two neighboring portal venular branches, there are cases in which only one side of the septum is connected to a vascular branch, whereas the other is supplied by another septum (compare *arrows* in Fig. 3). Yet another possibility can be seen in unit 14 (Fig. 3), in which the vascular septa are connected only on one side, either to a vascular branch or to a vascular septum, resulting in only a partial subdivision of the unit.

TABLE 2. Volumes of Sinusoidal Segments

Unit	Volumes of Sinusoidal Segments (nL) *Relative to Segment 6*						Total
	1	2	3	4	5	6	
1	28 *5.6*	22 *4.4*	17 *3.4*	13 *2.6*	9 *1.8*	5 *1.0*	94
2	45 *5.6*	36 *4.5*	29 *3.6*	22 *2.8*	15 *1.9*	8 *1.0*	155
3	39 *4.9*	31 *3.9*	26 *3.3*	20 *2.5*	13 *1.6*	8 *1.0*	137
4	46 *4.6*	37 *3.7*	30 *3.0*	23 *2.4*	16 *1.6*	10 *1.0*	162
5	57 *4.8*	47 *3.9*	37 *3.1*	29 *2.4*	20 *1.7*	12 *1.0*	202
6	91 *5.1*	73 *4.1*	59 *3.3*	45 *2.5*	32 *1.8*	18 *1.0*	318
7	95 *5.0*	77 *4.1*	62 *3.3*	47 *2.5*	32 *1.7*	19 *1.0*	332
8	73 *5.2*	59 *4.2*	47 *3.4*	36 *2.6*	25 *1.8*	14 *1.0*	254
9	46 *5.1*	35 *3.9*	29 *3.2*	22 *2.4*	15 *1.7*	9 *1.0*	156
11	80 *4.7*	68 *4.0*	55 *3.2*	42 *2.5*	30 *1.8*	17 *1.0*	292
12	69 *3.5*	58 *2.9*	47 *2.4*	38 *1.9*	28 *1.4*	20 *1.0*	260
Mean ± SEM	61 ± 7	49 ± 6	40 ± 5	31 ± 4	21 ± 3	13 ± 2	215
Mean ± SEM	*4.9 ± 0.2*	*4.0 ± 0.1*	*3.2 ± 0.1*	*2.5 ± 0.1*	*1.7 ± 0.0*	*1.0*	

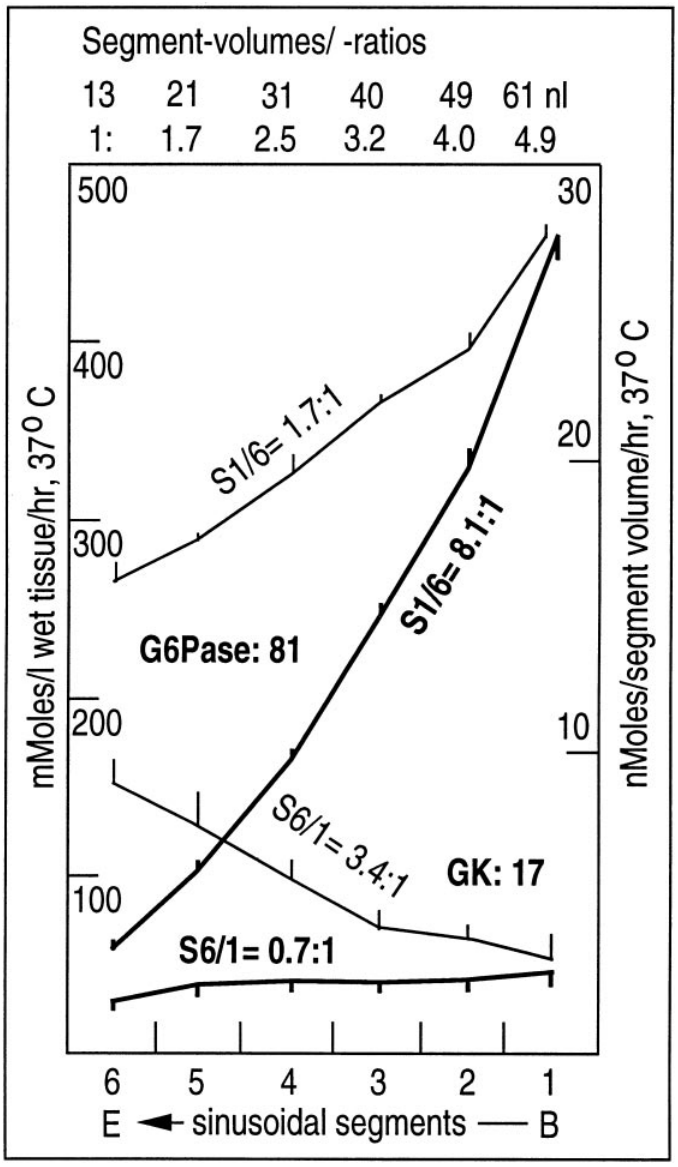

FIG. 8. Distribution of glucokinase (GK) and G6Pase activity in female rat liver. *Thin lines* and left *y*-axis: enzyme activities expressed in millimoles of substrate converted per liter of wet tissue. *Thick lines* and right *y*-axis: enzyme activities expressed in nanomoles of substrate converted per volume of the segments. Mean values (of at least triplicate measurements) ± SEM. S1/6: activity ratio of G6Pase of segments 1 and 6. S6/1: activity ratio of GK of segments 6 and 1. *x*-Axis at the top: volumes of segments 1 to 6 and volume ratios relative to segment 6. *x*-Axis at the bottom: sinusoidal distance subdivided into 6 segments, where segment 1 is located at the beginning (B) and segment 6 at the end (E). Numerals 81 and 17: G6Pase and GK activity expressed as nanomoles of substrate converted per 215 nL of wet tissue, *i.e.*, the total volume of the primary unit.

This subdivision by portal vessels and vascular septa closely follows the branching of the draining central venular tree, where the supplying vessels and septa keep a distance of about 170 µm, on average, from the bifurcations of the central venular tree (this is also true in areas in which a central venular branch exits through the surface of a group of primary units). The apparent distance varies with the actual section plane, *i.e.*, depends on the angle at which the sinusoids are sectioned. In view of this variability, we have chosen to take the section plane in which the draining central venules fuse as the horizontal border between primary units, because it can be accurately determined and because it takes into account to where the sinusoidal blood is drained.

The fact that the reconstructed secondary unit is located at the organ surface makes future studies neccessary to investigate whether and to what extent there are differences between units located close to and farther away from the surface. In addition, it is not clear at this point to what extent the reconstructed unit is reflecting the principle of subdivision of liver parenchyma in the rat. Current reconstruction studies indicate that the assembling of primary units is variable. So far, there is evidence for separate primary units and for groups of 3, 4, and 5 primary units integrated into a secondary unit. It also seems likely that more than 14 primary units can make up a secondary unit.

The primary units have a common but variable architecture. Each of the units was supplied by several (3 to 7) portal tracts, *i.e.*, branches of portal veins with diameters from 28 to 61 µm. These were oriented preferentially along the vertical axis of the units. Neighboring vessels were connected by vascular septa, giving most of the units a tri- to heptahedral shape (the units 10 and 14 had a conical shape). The size of the individual faces varied between 0.031 and 0.680 mm^2, and that of the total septal area (mantle) ranged from 0.932 to 3.016 mm^2. The primary units were 330 to 840 µm high and had volumes of 0.094 and 0.621 mm^3. The distance from the supplying surface of the units to the draining central venule (apparent length of sinusoids) was 355 ± 3 µm, on average. Portal sinusoids of 383 ± 3 µm were longer than septal sinusoids (326 ± 2 µm). In most of the units, sinusoidal blood was drained by a single central venular branch that was oriented along the vertical axis of the unit, *i.e.*, parallel to the supplying portal vessels. Units 10, 13, and 14 were drained by additional small branches of a main central venular branch. The diameter of the draining vessels ranged from 62 to 216 µm.

With regard to the basic organization, the primary units reconstructed from the liver of the rat are comparable with the lobular units of human and pig liver.[7,13,14,38] At the same time, there are two differences between the units: one is the abundance of connective tissue incorporated into the vascular septum of the unit in the pig, and its scarcity in human and rat liver; the second difference concerns the septal branches of portal veins that are present in human and pig liver, but not in the liver of the rat.

Concerning the nomenclature of the units, it should be mentioned that the terms "primary" and "secondary" units correspond to the terms "simple" and "compound" unit,[14] but appear to differ from the terminology of Matsumoto and Kawakami,[7] who have used the term "secondary" (*i.e.*, "classical") lobule as equivalent to "simple" lobule, and the term "primary" lobule to indicate the subdivision of "classical" lobules.

In previous studies, enzyme activity and metabolite levels were determined for six consecutive segments along the sinusoidal axis.[15,16,21] Sinusoidal gradients were calculated to assess the metabolic heterogeneity of hepatocytes, and thus to gain insight into the functional organization of liver parenchyma. From these studies, an organizational principle was detected, according to which synergistic enzymes are distributed similarly, whereas antagonistic enzymes (*e.g.*, G6Pase and glucokinase) are distributed in a reciprocal manner, thus leading to an intercellular compartmentation of opposing metabolic pathways. With regard to the metabolic organization of the parenchymal units, the present reconstruction study now offers the possibility of taking into account the three-dimensionality of the parenchymal units. From the numerical information on the volume of the different sinusoidal segments, it is evident that the segments, while covering equal lengths along the sinusoids, in

fact represent cell populations, the total volumes of which differ considerably, *i.e.*, by factors of up to 4.9.

To test the effect of taking into account the volumes of the different segments, we used previous microchemical data[17,18] on the gluco(neo)genic enzyme, G6Pase, and the glycolytic enzyme, glucokinase, which are distributed reciprocally along the sinusoidal axis. As indicated by the "linear" gradients, G6Pase activity decreases and that of glucokinase increases along sinusoids by 1.7- and 3.4-fold, respectively. The volumes of segments 1 to 5, on average, are larger by factors of 4.9, 4.0, 3.2, 2.5, and 1.7 than the volume of segment 6. From this, it follows that, based on the volume of the segments, there is in fact an 8.1-fold decrease in G6Pase activity from the perimeter to the center of the units. For the glucokinase reaction, the calculation shows that, because of the reciprocal slope of the "linear" enzyme gradient and the volume gradient, the values are rather similar in all of the segments. The volume-based data can also be used to determine enzyme activities of the parenchymal unit as a whole. Thus, total G6Pase activity of the primary unit amounts to 81 nmol per 215 nL of tissue per hour (equivalent to 377 mmol/L wet tissue per hour), and total glucokinase is 17 nmol per 215 nL tissue per hour (equivalent to 79 mmol/L wet tissue per hour). According to this calculation, the capacity for glucose release is 4.8-fold higher than that for the uptake of glucose.

This example indicates the value of considering the three-dimensionality of the parenchymal unit for an adequate functional interpretation of the metabolic heterogeneity of hepatocytes. Taking into account that hepatocytes at different locations represent cell populations of quite different sizes should also improve the interpretation of tissue sections. From the fact that hepatocytes at the beginning of the sinusoids (segment 1) represent an almost 5-fold larger cell population than those at the end (segment 6), it follows for the interpretation of distribution patterns of enzymes and other substances that even small changes at the beginning of the sinusoid may have a greater overall effect than extensive changes in hepatocytes at the ends of sinusoids. If the three-dimensionality of the parenchymal unit is not taken into consideration, it is likely that changes at the beginnings of sinusoids are underestimated, whereas those at the ends of sinusoids are overestimated (compare with Lamers[39]). This should also apply for the interpretation of sections from pathologically altered liver tissue.

Acknowledgment: This article is dedicated to Prof. em. T. Matsumoto, Department of Pathology, Jikei University, Tokyo, Japan. The authors are grateful to J. and F. Steel for their assistance with the manuscript.

REFERENCES

1. Kiernan F. The anatomy and physiology of the liver. Philos Tr Roy Soc Lond 1833;123:711-770.
2. Pfuhl W. Form und Gefaeβbeziehungen der Leberlaeppchen beim Menschen. Z Anat Entwicklgesch 1922;66:361-384.
3. Mall F. A study of the structural unit of the liver. J Anat 1906;5:227-308.
4. Rappaport AM, Borowy ZJ, Lougheed WM, Lotto N. Subdivision of hexagonal liver lobules into a structural and functional unit. Anat Rec 1954;119:11-34.
5. Sasse D: Liver structure and innervation. In: Thurmann RG, Kauffman FC, Jungermann K, eds. Regulation of Hepatic Metabolism. New York, London: Plenum, 1986;3-25.
6. Sasse D, Spornitz UM, Maly IP. Liver architecture. Enzyme 1992;46:8-32.
7. Matsumoto T, Kawakami M. The unit-concept of hepatic parenchyma. A re-examination based on angioarchitectural studies. Acta Pathol Jpn 1982;32(Suppl 2):285-314.
8. Quistorff B, Rømert P. High zone-selectivity of cell permeabilization following digitonin-pulse perfusion of rat liver. A re-interpretation of microcirculatory zones. Histochemistry 1989;92:487-498.
9. Lamers WH, Hilberts A, Furt E, Smith J, Jonges GN, van Noorden CJF, Gaasbeek et al. Hepatic enzymic zonation: a reevaluation of the concept of the liver acinus. HEPATOLOGY 1989;10:72-76.
10. Rømert P, Quistorff B, Behnke O. Histological evaluation of the zonation of colloidal gold uptake by the rat liver. Tissue Cell 1993;25:19-32.
11. Bhunchet E, Wake K. The portal lobule in rat liver fibrosis: a re-evaluation of the liver unit. HEPATOLOGY 1998;27:481-487.
12. Wuensche A. Zur Lupenanatomie der klassischen Leberlaeppchen des Schweines. Zbl Vet Med C Anat Histol Embryol 1981;10:342-350.
13. Wuensche A. Leberlaeppchen und portale Gefaesscheide beim Schwein. In: Parey P, ed. Adv Vet Med. Berlin: Scientific Publishers, 1988:1-117.
14. Ekataksin W, Wake K. Liver units in three dimensions. I. Organization of argyrophilic connective tissue skeleton in porcine liver with particular reference to the "compound hepatic lobule." Am J Anat 1991;191:113-153.
15. Teutsch HF. Regionality of glucose-6-phosphate hydrolysis in the liver lobule of the rat: metabolic heterogeneity of "portal" and "septal" sinusoids. HEPATOLOGY 1988;8:311-317.
16. Teutsch HF, Altemus J, Gerlach-Arbeiter S, Kyander-Teutsch TL. Distribution of 3-hydroxybyturate dehydrogenase in primary lobules of rat liver. J Histochem Cytochem 1992;40:213-219.
17. Teutsch HF. Quantitative histochemical assessment of regional differences in hepatic glucose uptake and release. Histochemistry 1985;82:159-164.
18. Teutsch HF, Lowry OH. Sex specific regional differences in hepatic glucokinase activity. Biochem Biophys Res Commun 1982;106:533-538.
19. Gershbein LL, Elias H. Observations on the anatomy of the rat liver. Anat Rec 1954;120:85-98.
20. Teutsch HF. Improved method for the histochemical demonstration of glucose-6-phosphatase. Histochemistry 1978;57:107-117.
21. Teutsch HF. Chemomorphology of liver parenchyma. Qualitative distribution patterns and quantitative sinusoidal profiles of G6Pase, G6PDH and malic enzyme and of glycogen content. Prog Histochem Cytochem 1981;14/3:1-92.
22. Winer BJ. Statistical Principles in Experimental Design. New-York: McGraw-Hill, 1971:149-260.
23. Teutsch HF. Sex-specific regionality of liver metabolism during starvation; with special reference to the heterogeneity of the lobular periphery. Histochemistry 1984;81:87-92.
24. Rappaport AM. The microcirculatory acinar concept of normal and pathological hepatic structure. Beitr Path 1976;157:215-243.
25. Jungermann K, Sasse D. Heterogeneity of liver parenchymal cells. Trends Biochem Sci 1978;3:198-202.
26. Hildebrand R, Schleicher A. Image analysis of the histochemical demonstration of glucose-6-phosphatase activity in rat liver. Histochemistry 1986;86:181-190.
27. Goergens HW, Hildebrand R, Haubitz I. Distribution pattern of alanine aminotransferase activity in rat liver. Histochemistry 1988;88:383-386.
28. Matsumoto T, Komori R, Magara T, Ui T, Kawakami M, Tokuda T, Takasaki S et al. A study on the normal structure of the human liver, with special reference to its angioarchitecture. Jikeikai Med J 1979;26:1-40.
29. Debeyre A. Morphology du lobule hépatique. Bibl Anat 1910;19:249-263.
30. Debeyre A. Circulation porte du lobule hépatique. Bibl Anat 1912;22:189-225.
31. Pfuhl W. Die Leber. In: von Moellendorf, ed. Handbuch der mikroskopischen Anatomie des Menschen. Vol 5. Berlin: Springer Verlag, 1932:235-425.
32. Pfuhl W. Ueber den Laeppchenbau der menschlichen Leber. Anat Anz 1922;55(Erg H):103-109.
33. Wuensche A, Preuss F. Pfortaderkoerbchen um Leberlaeppchen beweisen die Laeppchengliederung der Leber. Acta Anat 1986;125:32-36.
34. Welsch U. Histologie. 4th ed. Muenchen, Wien, Baltimore: Urban & Schwarzenberg, 1997:152.
35. Bucher O, Wartenberg H. Cytologie, Histologie und mikroskopische Anatomie des Menschen. 12th ed. Bern: Huber, 1997:296-303.
36. Elias H, Popper H. Venous distribution in livers. A M A Arch Pathol 1955;59:332-340.
37. Hase T, Brim J. Observation on the microcirculatory architecture of the rat liver. Anat Rec 1966;156:157-174.
38. Zou Z, Ekataksin W, Wake K. Zonal and regional differences identified from precision mapping of vitamin A–storing lipid droplets of the hepatic stellate cells in pig liver: a novel concept of addressing the intralobular area of heterogeneity. HEPATOLOGY 1998;27:1098-1108.
39. Lamers WH, Geerts WJC, Jonker A, Verbeek J, Wagenaar GTM, Moorman AFM. Quantitative graphical description of portocentral gradients in hepatic gene expression by image analysis. HEPATOLOGY 1997;26:398-406.